Reinforced glass concept: an experimental research

P.C. Louter, G.J. Hobbelman, F.A. Veer
Faculty of Architecture, Delft University of Technology, the Netherlands

ABSTRACT: The Glass & Transparency research group has developed a safety concept for structural glass beams which shows some analogy with reinforced concrete. Annealed float glass beams are reinforced by adhesively bonding a stainless steel section to the layout of the beam. Current research focuses on the effect of different reinforcement layouts and different adhesive types on the post-failure behaviour of reinforced glass beams. For this research 30 specimens with a length of 1.5 m have been subjected to a four-point bend test. Three reinforcement layouts and two adhesives (DELO GB368 and Araldite 2013) have been tested. The test results show differences in fracture patterns, failure behaviour and failure mechanisms for the tested reinforcement layouts and applied adhesives. Regarding structural qualities and consistency layout III and Araldite 2013 performed best. However, DELO GB368 provides some major advantages at the manufacturing process. Combining the advantages of both adhesives into one adhesive seems preferable.

1 INTRODUCTION

In contemporary architecture there is an increasing demand for transparent buildings and structures. Glass is desired as a load bearing material for structural components such as columns and beams. However, due to its brittleness and sudden failure behaviour, glass is considered a structurally unsafe material. At the faculty of Architecture, Delft University of Technology, the Zappi Glass & Transparency research group focuses on the development of transparent components and structures with safe failure behaviour. The research group has developed a safety concept for structural glass beams which shows some analogy with reinforced concrete. Annealed float glass beams are reinforced with a stainless steel section which is integrated in the layout of the beam and rigidly bonded to the glass.

Upon overloading the glass will crack but crack propagation will be limited due to the dissipation of fracture energy by deformation of the reinforcement. Furthermore the stainless steel section will act as a crack bridge carrying the tensile forces after the glass has cracked. Together with the compression force in the (un-cracked) compression zone an internal couple will be generated and the beam will still be able to carry load, see figure 1. In practice this will provide bystanders time to flee or to take measures. This concept has been developed in preceding research by Veer (2005) and successfully tested in previous beam designs up to a length of 7.2 m by Louter (2005).

The post-failure behaviour of a reinforced glass beam is highly dependent on the bond between glass and reinforcement. Current research focuses on the effect of different reinforcement layouts and different adhesive types on the post-initial failure behaviour of reinforced glass beams. For this research 30 specimens with a length of 1.5 m have been subjected to a four-point bend test. Three different reinforcement layouts (I, II and III) and two different adhesives (DELO GB368 and Araldite 2013) have been tested.
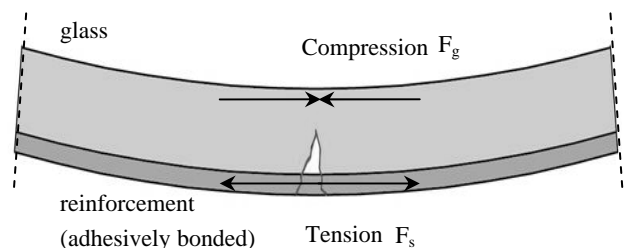
Figure 1. Reinforced glass beam concept: schematic overview of distribution of forces after glass failure.

2 REINFORCEMENT LAYOUTS

The tested reinforcement layouts are displayed in figure 2. For each layout an annealed float glass beam of 1500*115*10 mm is applied.

- Layout I consists of two stainless steel sections (each 2*9 mm) which are bonded to the side panes of the glass beam.
- Layout II consists of a stainless steel box section (10*10*1 mm) which is bonded to the edge of the glass beam.
- Layout III consists of a stainless steel box section (10*10*1 mm) which is bonded to the edge of the glass beam and encapsulated by two additional outer layers (each 40*6 mm). These outer layers are bonded to the side panes of the glass beam (using the transparent DELO GB368 adhesive).
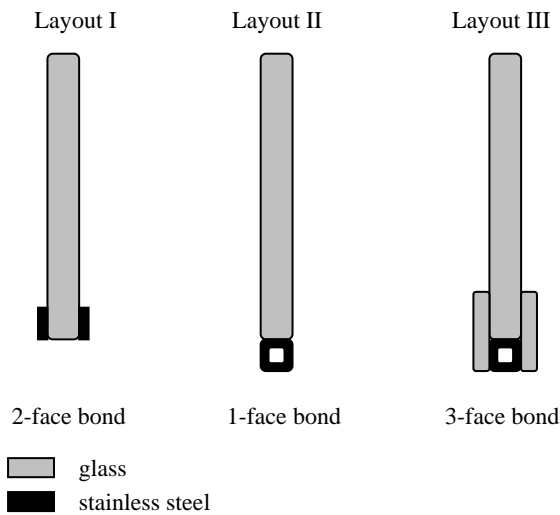
Figure 2. Tested reinforcement layouts.
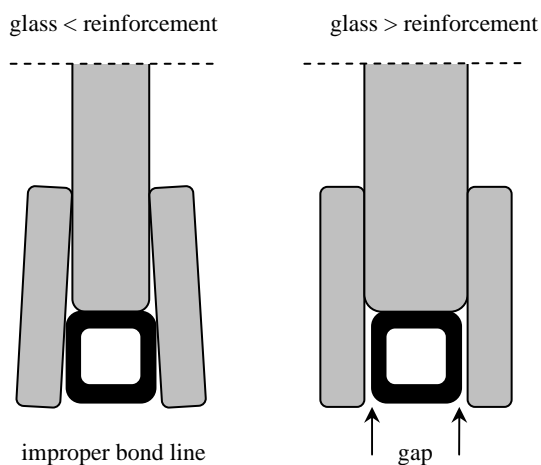
Figure 3. Effects of dimensional inaccuracies for layout III.

The amount of steel in the section is equal for each layout; the area of the box section (36 mm^2) is equal to the area of both full sections (2* 2*9 mm = 36 mm^2). The developed reinforcement layouts differ in two important aspects:

a. bond area (*1-, 2- or 3*-face bond)

The interaction between glass and reinforcement is fully dependent on the adhesive bond. Forces are transferred via shear in the adhesive layer. Upon glass failure large tensile forces (in the reinforcement) have to be transferred from and to the glass. The bond area of the tested reinforcement layouts differ in 1-, 2- or 3-face bond, see figure 2. Enlarging the bond area will reduce shear stresses in the adhesive bond and will prevent from premature detachment of reinforcement. In this respect layout III, which has the largest bond area, should perform best.

b. capacity to adapt to dimensional inaccuracies

The strength of an adhesive bond is, amongst other aspects, dependent on the thickness of the bond layer. Generally a thin adhesive layer will result in a strong bond. For reinforcement layout I and II the thickness of the adhesive bond can be controlled during the bonding process. By clamping the reinforcement to the glass any adhesive surplus will be pressed out. However, for reinforcement layout III this can not be done since the reinforcement is bonded *between* two glass sheets. In this case the thickness of both vertical bond layers depends on to what extent the dimensions of the reinforcement correspond with the thickness of the inner glass layer. Any dimensional inaccuracy in glass and/or reinforcement will result in a deviating bond thickness. In case the glass is *thinner* than the reinforcement an improper bond line occurs, see figure 3. In case the glass is *thicker* than the reinforcement the bond layer will have to be thicker and the applied adhesive will have to be capable of filling this gap while maintaining its strength. According to the European standard EN 572-2 the allowed tolerances for float glass with the applied glass thickness of 10 mm are ± 0.3 mm.

3 ADHESIVE TYPES

Each reinforcement layout has been tested for two different adhesives, DELO GB368 (abr. GB368) and Araldite 2013 (abr. AR2013). The most important properties of these adhesives are listed in table 1. A short description of both adhesive is provided in the following paragraphs.

3.1 *DELO Photobond GB368*

The acrylic based photo-initiated curing adhesive DELO GB368 has been developed for glass-glass and glass-metal bonding. In previous reinforced glass beam designs, which consist of multiple glass layers and stainless steel reinforcement, this adhesive has already been applied for both glass-glass and glass-reinforcement bonding.

For the bonding process of (multi-layer) reinforced glass beams DELO GB368 provides three main *advantages*;

a) Polymerization is only initiated by UV-radiation, which enables an accurate positioning of the substrates without being rushed by curing times,

b) The adhesive cures within 30 seconds which limits production time,

c) Glass-glass and glass-reinforcement bonding can be executed simultaneous, since the same adhesive is applicable for both purposes.

The main *disadvantages* of this adhesive for the reinforced glass concept are:

a) The adhesive has to be cured with a maximum thickness of 0.1 mm and is not able to fill gaps caused by dimensional inaccuracies,

b) Preceding experimental research showed the adhesive is only limited resistant to shock loads which occur upon glass failure, causing premature collapse of the beam.

3.2 *Araldite 2013*

Although the two-component epoxy Araldite 2013 has been developed as a metal bonding adhesive it is also suitable for bonding other materials such as ceramics, rubbers, rigid plastics and glass. Although the Araldite has not yet been applied in the reinforced glass conept this adhesive might provide some *advantages*:

a) According to the manufacturer's datasheets Araldite 2013 has a filling capacity up to 5 mm, which should make it suitable for taking up any dimensional inaccuracies,

b) The Araldite is a rather tough adhesive, which should make it more resistant to the shock loads, which occur upon glass failure.

The main *disadvantages* for the reinforced glass concept of the Araldite 2013 seem to be:

a) Since this adhesive is not suitable for glass-glass bonding (due to its grey colour) the reinforced glass bonding process has to be divided in two stages; the glass-glass bonding has to be executed with a different (transparent) adhesive than the glass-reinforcement bonding, which will increase production time.

b) The adhesive has a limited handling time of about 1 hour after the two components have been mixed; accurate positioning of the substrates has to be completed within this time span,

c) At room temperature the adhesive has a curing time of 4 hours to reach a light handling strength of 1 N/mm^2, and a curing time of 10 hours to reach 50% of the final shear strength. Due to this long curing time the substrates have to be clamped for several hours, which will increase production time.

Table 1. Key properties of DELO GB 368 and Araldite 2013, according to the manufacturer's datasheets.

		DELO GB 368	Araldite 2013
		Acrylic based	Two-component epoxy
Shear strength	[MPa]	23 (glass-glass) 23 (glass-alu)	18
Viscosity	[mPas]	5700	Thixotropic (mixed) Gap filling capacity up to 5 mm
Colour		Transparent	Grey
Curing time		Minimum curing time 15 seconds	4 hours at 23°C to reach 1 MPa. 10 hours at 23°C to reach 10 MPa.

4 TEST RESULTS

Of each layout (LI, LII and LIII) and for both adhesives (GB368 and AR2013) 5 specimens have been made, which results in a total of 30 specimens. All specimens have been subjected to a 4-point bend test to validate their structural behaviour. For this test a Zwick 100 kN test rig was provided with a steel hinge-and-roller-support rig. Supports were 1400 mm apart, loads were 400 mm apart and lateral (anti-buckling) supports were 550 mm apart. The specimens were loaded at a rate of 1 mm/minute and loading was continued until total destruction. Load and vertical displacement were monitored. The specimens were provided with a grid, which enables visual monitoring of crack heights. All tests were captured on video.

4.1 *General failure behaviour*

First of all the general failure process of all specimens will be described in this paragraph. The specific failure behaviour for each layout and adhesive type will be discussed in proceeding paragraphs.

The stress-displacement diagrams for each layout and adhesive type are given in figures 5, 6, 9, 10, 13 and 14. A general and schematic stress-displacement diagram is given in figure 4. Three general stages/phases can be distinguished:

a. Linear elastic behaviour

All specimens showed a linear elastic behaviour until at a global tensile bending stress at the lower edge of the glass of 30 – 65 N/mm^2 a first crack occurred. This crack originated at the lower edge of the glass beam and ran about 2/3 of the total beam height before being stopped in the upper compression zone. Due to the sudden increase in vertical displacement of the specimen the load dropped.

b. post-failure behaviour / residual strength

As loading was continued the load started to rise again until at a second peak-load another crack occurred causing a drop in load. This process might be repeated one or several times. The stress-displacement diagram shows a decrease in beam stiffness after each peak-load. For most specimens the residual strength exceeded the initial failure load.

c. total failure

Final failure (point c) occurred due to either,

- Progressive detachment of reinforcement; adhesive failure, or
- Lateral torsional buckling; lateral instability of the compression zone due to increasing crack growth and increasing compression forces.
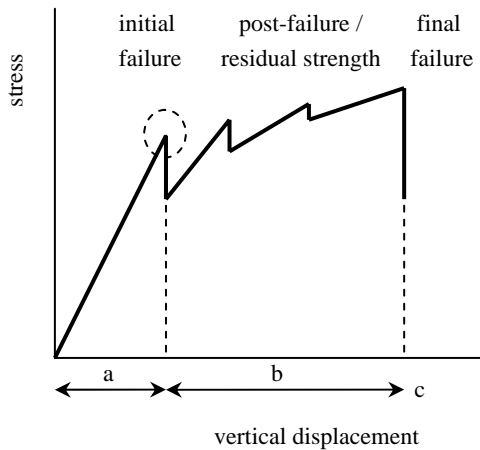
Figure 4. Schematic stress-displacement diagram for all reinforcement layouts.

4.2 Layout I

The stress-displacement diagrams of layout I specimens for both adhesives are given in figures 5 and 6. Regardless of the applied adhesive, all specimens of layout I showed comparable bending stiffness in the linear elastic phase. After initial failure the specimens showed a small increase in load of -15 to +64% and a rather large increase in vertical displacement of 214 - 675%.
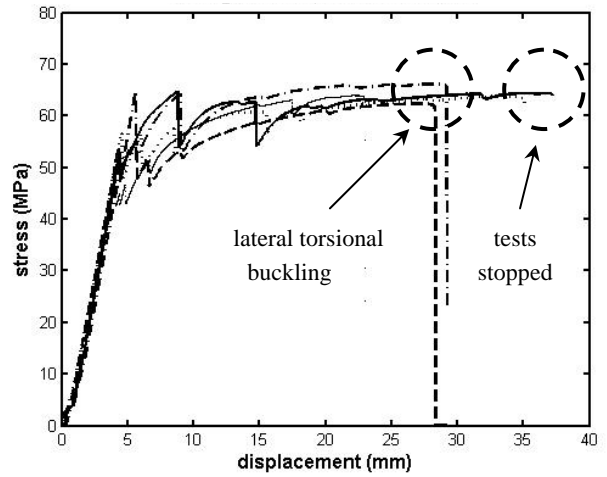
Figure 5. Stress-displacement diagram of layout I - GB368 specimens.
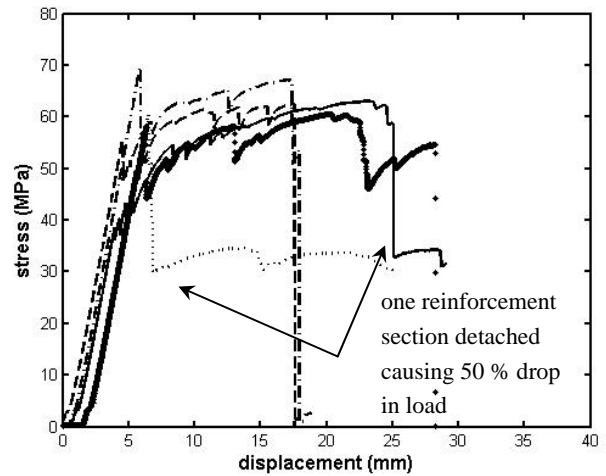
Figure 6. Stress-displacement diagrams of layout I - AR2013 specimens.

4.2.1 L I - GB368 - specimens

Figure 7 gives a schematic overview of the crack propagation at different time steps (1-4) for layout I-GB368 specimens. Upon overloading a V-shaped crack with a height of 75-90 mm occurred (1). As loading was continued a second or even third V-shaped crack occurred (2). Subsequently the cracks started to propagate horizontally and started to grow towards each other (3). Although smaller cracks occurred at the outline of the compression zone a compression zone of 10-15 mm remained un-cracked (4) until the beam failed due to lateral torsional buckling. For three specimens the test was stopped due to extensive vertical displacements, see figure 5.
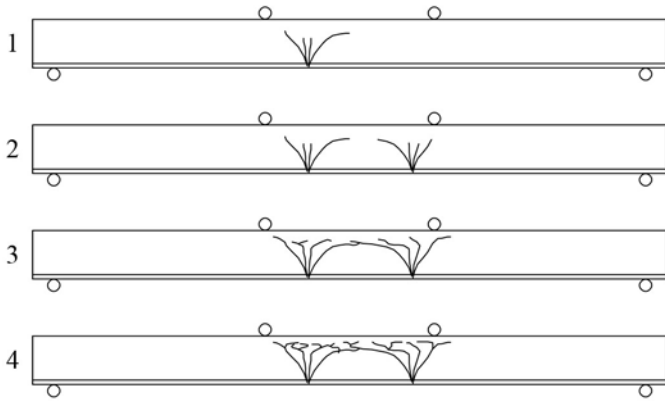
Figure 7. Schematic overview of crack propagation, at different time steps (1-4), for L I – GB368 specimens.

Figure 8. Schematic overview of crack propagation, at different time steps (1-4), for L I – AR2013 specimens.

4.2.2 *L I - AR2013 - specimens*

Figure 8 gives a schematic overview of the crack propagation at different time steps (1-4) for layout I-AR2013 specimens. At the initial failure load a V-shaped crack with a height of 80 mm occurred (1) which started to propagate horizontally (2) as loading was continued. Subsequently multiple V-shaped cracks occurred (3). Gradually the reinforcement started to detach at mid-span and the glass started to slide past the reinforcement (4). For two specimens one of the reinforcement sections detached at one beam end, causing a 50% drop in load, see figure 6.

Finally the specimens failed due to detachment of both reinforcement sections at one beam end. For two specimens the residual strength did not exceed the initial failure load.

4.3 *Layout II*

The stress-displacement diagrams of layout II specimens for both adhesives are given in figures 9 and 10. Except for two LII-GB368 specimens all specimens show comparable bending stiffness. After initial failure the specimens show an increase in load of -25 to +94% and a relatively small increase in vertical displacement of 27 – 225%.

4.3.1 *L II - GB368 - specimens*

Figure 11 gives a schematic overview of the crack propagation at different time steps (1-4) for layout II-GB368 specimens. Upon overloading a V-shaped crack with a rather dense fracture pattern and a height of 70-80 mm occurred (1). As loading was continued a second crack occurred for some specimens. Subsequently the V-shaped crack(s) started to propagate in a horizontal manner (2/3). Finally all specimens failed due to detachment of reinforcement at one beam end. The specimens showed a 'bull-bar' shaped crack pattern (4).

For one specimen the residual strength did not exceed the initial failure load.
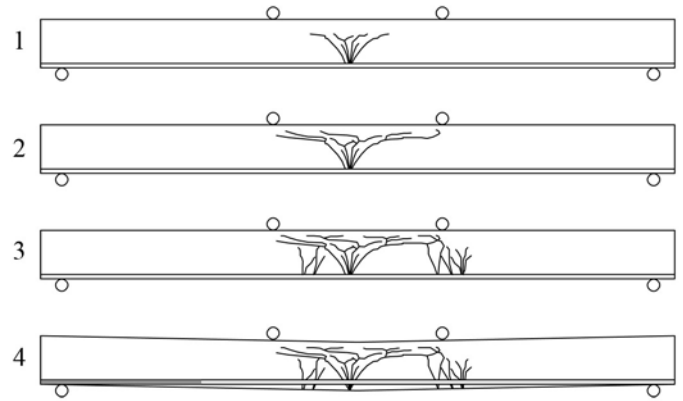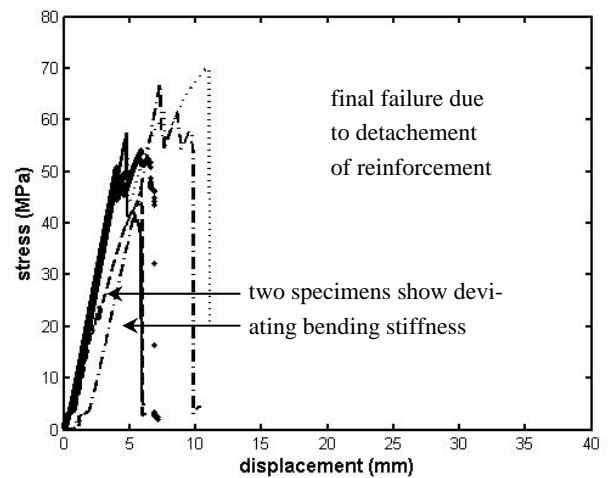
Figure 9. Stress-displacement diagram of layout II - GB368 specimens.
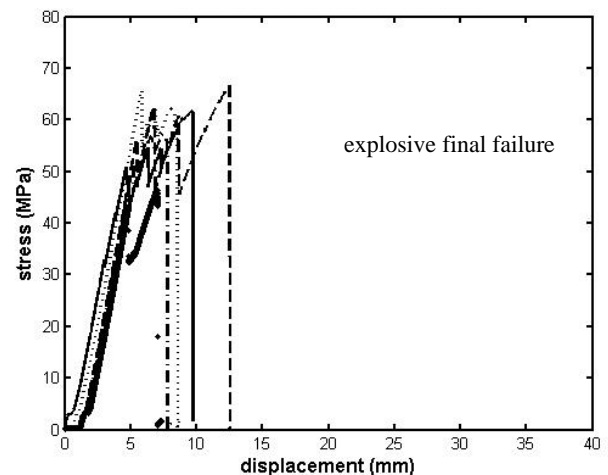
Figure 10. Stress-displacement diagram of layout II - AR2013 specimens.
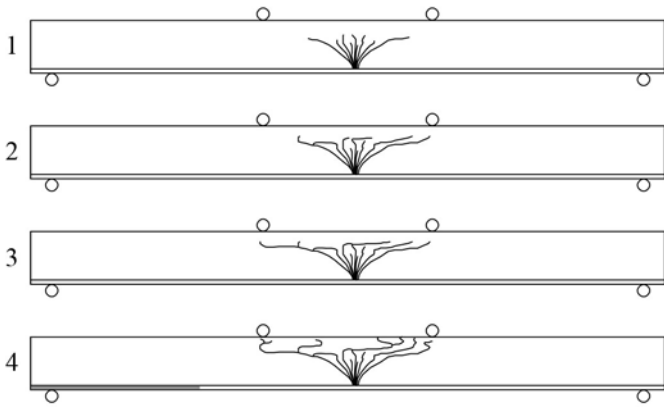
Figure 11. Schematic overview of crack propagation, at different time steps (1-4), for L II – GB368 specimens.

Figure 12. Schematic overview of crack propagation, at different time steps (1-4), for L II – AR2013 specimens.

4.3.2 *L II - AR2013- specimens*

Figure 12 gives a schematic overview of the crack propagation at different time steps (1-4) for layout II-AR2013 specimens. Upon overloading a V-shaped crack with a height of 70-80 mm occurred (1). This crack has fewer branches as was observed for LII-GB368 specimens. As loading was continued multiple V-shaped cracks occurred (2). The cracks seemed to be 'non-related' and they did not grow towards each other. Subsequently small diagonal/sloped cracks occurred towards the beam end (3). Finally the specimens failed rather explosive. At the beam end large cracks were observed and the reinforcement had largely been torn from the glass (4). However, small glass particles remained attached to the reinforcement.

For one specimen the residual strength did not exceed the initial failure load.

4.4 *Layout III*

The stress-displacement diagrams of layout III specimens for both adhesive are given in figures 13 and 14. All specimens show comparable bending stiffness and large vertical displacements. After initial failure the specimens show an increase in load of +26 to +84% and a large increase in vertical displacement of 240 – 401%.

4.4.1 *L III – GB368 – specimens*

Figure 15 gives a schematic overview of the crack propagation at different time steps (1-4) for layout III – GB368 specimens. Upon overloading a V-shaped crack with a height of 80-90 mm occurred (1). As loading was continued a second or even a third V-shaped crack occurred (2). These cracks propagated horizontally and tended to overlap (3). At the upper edge of the beam a zone of 30 mm remained un-cracked. Finally the upper zone at midspan failed rather explosive due to lateral torsional buckling (4).
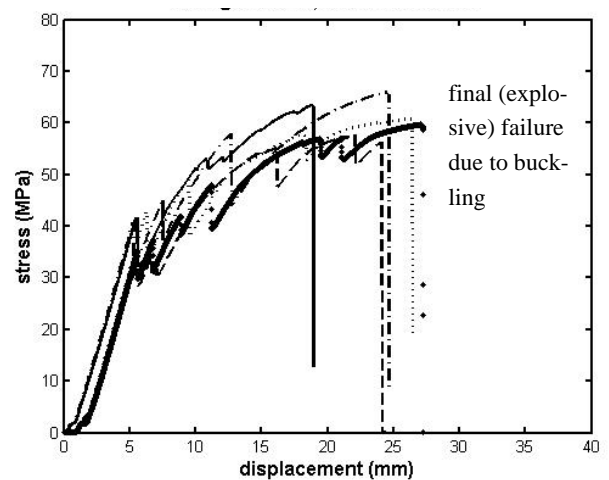
Figure 13. Stress-displacement diagram of layout III - GB368 specimens.
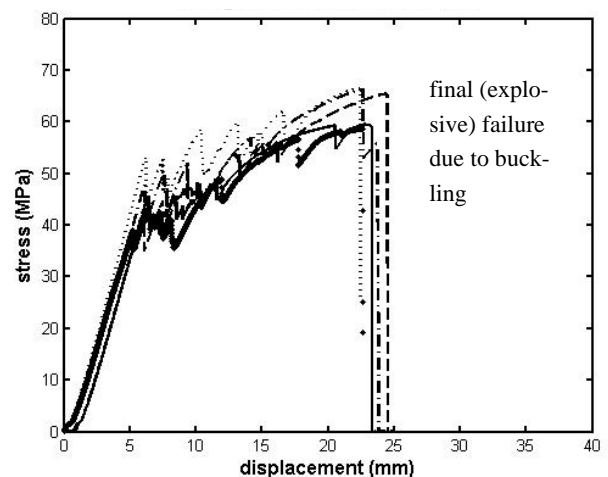
Figure 14. Stress-displacement diagram of layout III - AR2013 specimens.
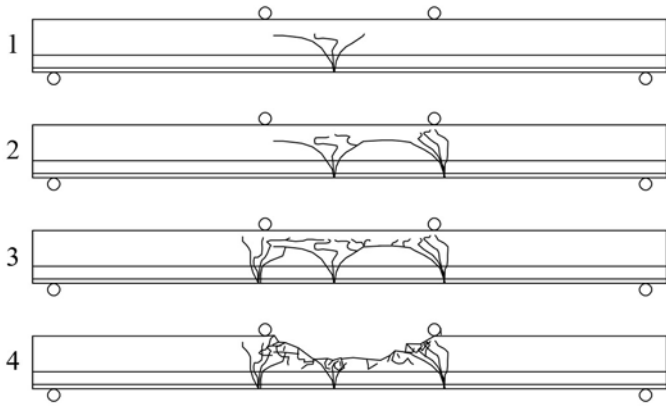
Figure 15. Schematic overview of crack propagation, at different time steps (1-4), for L III – GB368 specimens.

4.4.2 L III – AR2013 – specimens

Figure 17 gives a schematic overview of the crack propagation at different time steps (1-4) for layout III – AR2013 specimens. Upon overloading one or multiple V-shaped cracks with a height of 90-95 mm occurred (1). As loading was continued the existing cracks remained rather stable and successively multiple cracks occurred (2/3). At the upper edge of the beam a zone of 30 mm remained un-cracked. Finally the specimens failed explosive due to lateral torsional buckling.

5 DISCUSSION

The test results show differences in fracture patterns, failure behaviour and failure mechanisms for the tested reinforcement layouts and the applied adhesives. The results will be discussed by layout and adhesive type.

5.1 Layouts

Figure 16 shows a schematic stress-displacement diagram/tendency of all three tested reinforcement layouts.
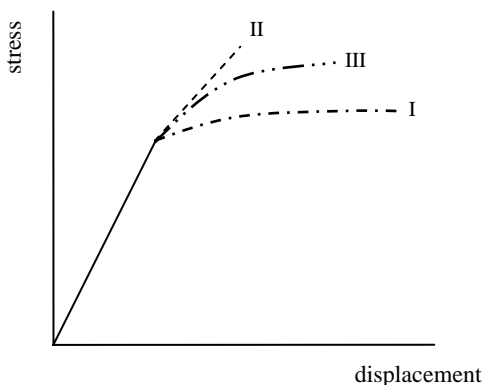
Figure 16. Schematic stress-displacement diagram of layout I, II and III.
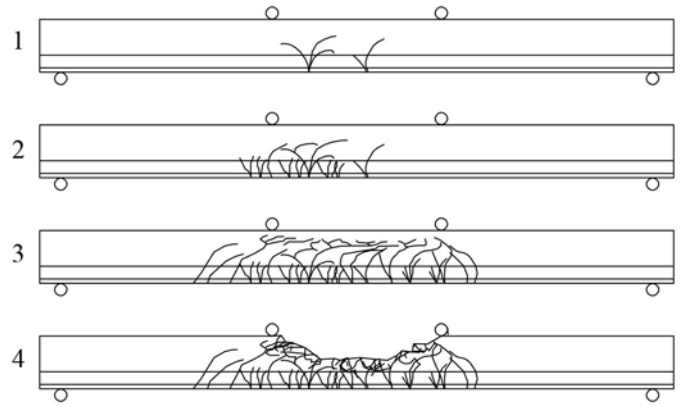
Figure 17. Schematic overview of crack propagation, at different time steps (1-4), for L III – AR2013 specimens.

The layouts show different post-failure trajectories:

Layout I shows an elastic ideal plastic behaviour. After initial failure bending stiffness is strongly reduced. The specimens show a large deformation capacity, but only a small capability of carrying increasing loads. This might be caused by local detachment of reinforcement, which allows for large deformations since the glass can 'slide' past the reinforcement. Local detachment of reinforcement or even full detachment of one reinforcement section did not lead to a full collapse of the specimens, see figure 6. Due to the large bond area and the application of two reinforcement sections a preferable redundancy has been built in, which contributes to safe failure behaviour.

Layout II shows the most brittle behaviour. After initial failure a limited decrease in bending stiffness is observed and the beams are able to carry increasing loads. For this layout all specimens failed due to detachment of reinforcement (adhesive failure). This can be explained by the limited bond area between glass and reinforcement, which leads to high shear stresses. For layout I only a 1-face bond is applied, which excludes any redundancy. Upon failure of this single bond face fails there is no second bond face to limit this failure or to carry the forces. In this respect this layout option is the least preferable.

Layout III shows an elastic / strain hardening behaviour. After a first crack occurs bending stiffness gradually decreases, but the beams are still able to carry extensive and increasing loads. The large bond area in this beam layout (3-face bond) prevents from premature detachment of reinforcement. If one of the bond faces might fail (partially), there are still 2 bond faces left to carry the tensile forces in the reinforcement, which provides redundancy and safe failure behaviour. Due to the proper bond detachment of reinforcement did not occur and the specimens were able to carry increasing loads. As the compression force in the glass increased lateral instability of the

compression zone became critical. Due to increasing crack growth the upper (un-cracked) compression zone detaches from the lower part and becomes susceptible to buckling. All specimens of layout III finally failed due to buckling. This failure mechanism has been observed in preceding research by Louter (2006) and is a determining factor in dimensioning (reinforced) glass beams according to Belis (2005).

The layout III-specimens showed consistent results. For all specimens the final failure load exceeded the initial failure load and the final failure mechanism was equal for each specimen. Cause of its consistency, built-in redundancy and safe failure behaviour this layout seems the most preferable regarding structural qualities.

5.2 *Adhesives*

The test results show a difference in fracture pattern for the AR2013 and GB368 specimens. Regardless of layout the GB368-specimens show *few*, but *large* cracks whereas the AR2013-specimens show *many,* but *small* cracks. This difference becomes most distinct for failure stage 3 of both LIII-AR2013 and LIII-GB368 specimens, see figures 15 and 17. The AR2013-specimens show a more dense fracture pattern than the GB368-specimens. This difference in fracture pattern can be explained by a difference in toughness of both adhesives. For GB368-specimens local de-bonding of reinforcement was observed at the crack tips/origin. The shock load which occurs upon glass fracture causes the adhesive to fail for several centimetres on either side of the crack tip. This local de-bonding of reinforcement allows for large crack opening displacements and extensive crack propagation. Due to the higher toughness of the AR2013-adhesive local de-bonding occurs to a lesser extend for the AR2013-specimens. Crack opening displacement and crack propagation are limited and stresses are more evenly/equally (re)distributed. The crack itself remains stable and new cracks will occur next to the existing crack.

Both adhesives have only been tested for single layer glass beams. In a multi-layer glass beam the occurrence of *few* but *large* cracks (as for GB368-specimens) might be more advantageous than the occurrence of *many* but *small* cracks (as for AR2013-specimens). In a multi-layer glass beam lateral instability due to overlapping cracks is more likely to occur for a dense (many small cracks) fracture pattern. In this respect the GB368-adhesive seems advantageous, but it is noted that further research is recommended.

The AR2013-specimens show more consistent results. For instance for layout III the scatter in ultimate vertical displacement of AR2013-specimens is less than of GB368-specimens. Due to its gap filling quality, the AR2013-adhesive is able to take up any dimensional inaccuracy, which leads to a more consistent structural quality. The structural performance of the AR2013-adhesive seems less dependent on irregularities at the manufacturing process than the GB368-adhesive. In this respect the AR2013-adhesive seems more preferable and generates more predictable and consistent failure behaviour than the GB368-adhesive. However, AR2013-adhesive has more limitations at the bonding process as has been noted in paragraph 3.2. A combination of both adhesives seems ideal: a transparent adhesive which is rapidly cured by UV-light, tough, resistant to shock loads, not sensitive to irregularities at the manufacturing process and applicable for both glass-glass and glass-reinforcement bonding.

The way an adhesive responds to irregularities at the manufacturing process is hard to take into account in a finite element model. Whether an adhesive is suitable for the reinforced glass concept is therefore hard to determine by numerical research and can only be determined by experimental research.

6 CONCLUSIONS

- Regarding structural quality reinforcement layout III, which has the largest bond area, is the most preferable, since this layout showed high residual strength and consistent results.
- Regarding structural quality adhesive Araldite 2013 is the most preferable adhesive for the reinforced glass concept, since this adhesive can adapt to dimensional inaccuracies and provided the most consistent results.
- Regarding the production process DELO GB368 is preferable because of its short curing time and its applicability for both glass-glass and glass-reinforcement bonding.
- Combining the structural and production advantages of both tested adhesives is preferable.

REFERENCES

Belis, J. 2005. Kipsterkte van monolithische en gelamineerde glazen liggers. *Dissertation, Laboratory for Research on Structural Models, Ghent University*.

Veer, F.A. 2005. 10 years of Zappi research. *Proceedings of 9th Glass Processing Days, Tampere, Finland*

Louter, P.C. & Belis, J. & Bos, F.P. & Veer, F.A. & Hobbelman G.J. 2005. Reinforced Glass Cantilever Beams. *Proceedings of 9th Glass Processing Days, Tampere, Finland.*

Louter, P.C. & Schetters L. & Veer, F.A. & Van Herwijnen, F. & Romein, T. 2006. Experimental research on scale 1:8 models of an 18 m reinforced glass beam. *Proceedings of the 2nd International Symposium on the Architectural Application of Glass. Munich, Germany.*

European Standard 2004. EN 572-2 Glass in Building –Basic Soda lime silicate glass products –part 2: Float glass.